Natural Resources for Human Health
eISSN: 2583-1194

Original Research

Received 22 May 2026
Revised 26 June 2026
Accepted 18 July 2026

Natural Resources for Human Health 2026, Vol. 6 (7s): 517–529

KEYWORDS:
Molecular graph, Neighborhood Topological Index, Graph Entropy, Augmented Zagreb Index, QSPR, Mixed-Ligand Copper(II) complex, SARS-CoV-2

Predicting Dual-Target Antibacterial Activity and SARS-CoV-2 Docking Affinity of Pendant-Armed Copper (II) Metallodrugs: A Neighborhood Topological and Graph Entropy Approach

Mythili V[1], S Shenbaga Devi[1,2], Padmanathan Arthi[3], S Dhanalakshmi[1],*

[1]Department of Mathematics, SRM Institute of Science and Technology Ramapuram Campus, Chennai - 600 089, India.
[2]Department of Mathematics, Loyola ICAM College of Engineering and Technology, Loyola Campus, Nungambakkam, Chennai - 600 034, India.
[3]Department of Chemistry, SRM Institute of Science and Technology Ramapuram Campus , Chennai - 600 089, India.

ABSTRACT: This study establishes a purely structural, laboratory-free framework for ranking the biomedical efficacy of discrete coordination compounds using advanced chemical graph theory. Focus is placed on six pendant-armed mixed-ligand copper(II) complexes, [CuL ^(1-3) (diimine)] (1-6), featuring varying degrees of nitro substitution and either 2,2'-bipyridyl or 1,10-phenanthroline co-ligands. By explicitly incorporating the central copper core and its seven coordinate bonds, we map the hydrogen-suppressed molecular graphs and compute eleven neighborhood-degree topological indices alongside their corresponding Shannon graph entropies. Multi-target quantitative structure-property relationship (QSPR) models were validated against experimental antibacterial activity (spanning eight bacterial strains) and molecular docking scores targeting the SARS-CoV-2 main protease. The Augmented Zagreb Index served as an exceptional single-descriptor predictor for mean antibacterial performance (R^2=0.969,F=123.9,p=0.0004, R^2_{LOO}=0.934), while size-type descriptors ⟦M⟧_1,HP) accurately captured the SARS-CoV-2 molecular-docking binding free energies ($R^2 \approx 0.78$). These findings demonstrate that neighborhood-sphere structural descriptors bypass intensive quantum-chemical optimization, offering a highly efficient and predictive route for accelerating the discovery and development of heteroleptic metallodrug candidates.

1. INTRODUCTION

Chemical graph theory represents a molecule as a graph $G = (V, E)$ in which the vertices stand for atoms and the edges for chemical bonds, and it associates with this graph a single real number, a topological index, that is invariant under graph isomorphism [1, 2]. Because such an index is obtained purely from connectivity, it can be computed without any laboratory measurement or quantumchemical optimisation, and yet it often correlates strongly with physicochemical and biological properties. This observation is the foundation of quantitative structure-property and structure-activity relationship (QSPR/QSAR) modelling, in which molecular descriptors are regressed against measured properties to build predictive, interpretable models. The field began with Wiener's distance-based index for the boiling points of paraffins [1] and with the Zagreb indices introduced by Gutman and Trinajić in their study of total π-electron energy [2], and it has since grown into one of the most active areas of mathematical chemistry.

The success of the early descriptors motivated a large family of degree-based indices, each emphasising a different structural feature. The Randić connectivity index weights every edge by the inverse square root of the product of its end-degrees and quantifies molecular branching [3]; the atom-bond connectivity (ABC) index was designed to model the stability and enthalpy of formation of alkanes [4]; the geometric-arithmetic (GA) index compares the geometric and arithmetic means of the end-degrees[5]; and the augmented Zagreb index (AZI), which raises a degree ratio to the third power, is among the most discriminating predictors of formation enthalpies [6]. More recently, Gutman introduced the Sombor index from a geometric interpretation of the degree pair [7], and the resulting Sombor family (including reduced and modified variants) has been developed intensively in the current literature [8], with explicit applications to main-group and coordination chemistry [9]. Together with the hyper-Zagreb and harmonic indices, these descriptors form the standard toolbox used below.

A limitation of the ordinary degree-based indices is that they see only the immediate degree of each bonded pair and are therefore insensitive to the wider environment of an edge. To capture this second-sphere information, Mondal, De and Pal introduced neighbourhood degree-based indices, in which every vertex is re-weighted by the sum of the degrees of its neighbours [10]. The neighbourhood descriptors, and the closely related NM-polynomial machinery, have proved to be markedly better predictors than their ordinary counterparts in a series of recent QSPR studies: on anti-HIV drugs [11], on asthma medications [12], on nanotubes and crystallographic networks [13] and on antiviral agents for COVID-19 [14]. This growing evidence base is a central reason for adopting the neighbourhood formulation in the present work alongside the classical indices.

A complementary way of summarising a molecular graph is through its entropy. Following Shannon's information-theoretic definition, a topological index can be turned into a probability distribution over the edge set, and the associated graph entropy then measures the structural heterogeneity or "complexity" encoded by that index [15]. Index-weighted graph entropies have been computed for a wide range of chemical systems in the last three years, including fractal and dendrimer-type molecular graphs [16], and they are increasingly reported together with the underlying indices in QSPR pipelines. Combining degree-based indices, neighborhood indices and their entropies within a single study, as we do here, therefore reflects current best practice in the field.

The QSPR/QSAR modelling of drug molecules by topological indices has expanded rapidly and now spans an unusually broad range of therapeutic areas. Within the last three years alone, index-based regression models have been reported for Lyme-disease medicines [17], hepatitis therapeutics [18, 19], potential antimalarial compounds [20], poisonous and medicinal alkaloids [21] and antiviral agents against SARS-CoV-2 [14]. These studies consistently show that a small number of degree- or neighbourhood based descriptors can reproduce measured physicochemical and biological endpoints with correlation coefficients above 0.9, and that leave-one-out cross-validation is a practical safeguard against overfitting on the modest data sets typical of a single chemical series. The methodology adopted in the present paper follows this now-established protocol.

By contrast, the graph-theoretical treatment of metal complexes remains comparatively underdeveloped. Most published QSPR work addresses purely organic drugs or extended inorganic networks such as metal-organic and covalent-organic frameworks [22]; discrete coordination complexes, in which the metal centre and its coordinate Cu-O and Cu-N bonds are an integral part of the molecular graph, have received far less attention. This is a notable gap, because mixed-ligand copper(II) complexes are of sustained interest as metallodrugs: copper is redox-accessible under physiological conditions, and heteroleptic complexes that combine a pendant-armed phenolate Schiff base with an $N-N$ diimine coligand (2,2'-bipyridyl or 1,10-phenanthroline) exhibit pronounced antibacterial activity, groove-mode DNA binding and, in recent docking studies, strong affinity for the SARS-CoV-2 receptor [23]. The six complexes examined here, 1-6, belong to exactly this class: they are built from 5-methylsalicylaldehydederived pendant-armed ligands $H_2\,L^{1-3}$ of increasing nitro substitution together with bipyridyl or phenanthroline co-ligands, and their synthesis, spectral characterisation and multi-target biological profile have been reported [23]. They therefore provide an ideal, experimentally well-characterised platform on which to test whether topological descriptors can rank the activity of coordination compounds.

Motivated by this gap, the present study pursues three objectives. First, we construct the hydrogen suppressed molecular graph of each of the six complexes, treating the copper centre and its seven coordinate bonds explicitly, and we determine the complete neighbourhood-degree edge partition of every graph. Second, from these partitions we evaluate eleven neighborhood topological indices, the corresponding responding ordinary degree-based indices and the neighborhood graph entropies, verifying that the edge partitions reproduce

the computed index values exactly. Third, we build and cross-validate single-descriptor QSPR models that link these descriptors to two independent experimental endpoints-the antibacterial activity against eight bacterial strains and the molecular-docking affinity towards the SARS-CoV-2 main protease - and we relate the descriptor ordering to the reported DNA-binding propensity. To our knowledge, this is the first graph-theoretical, multi-target QSPR analysis [24, 25] of a family of pendantarmed mixed-ligand copper(II) complexes.

2. MATHEMATICAL PRELIMINARIES

Let $G = (V, E)$ be the molecular graph of a complex; V is the set of non-hydrogen atoms and E the set of bonds, including the Cu-O and Cu-N coordinate bonds (Fig. 1). For $u \in V$, d_u is the degree of u and

$$\delta_u = \sum_{v \in N(u)} d_v$$

is the neighborhood degree of u, i.e. the sum of the degrees of its neighbours. The neighborhood degree based indices used here are obtained from the definitions of Table 1 by replacing each vertex degree d_u by its neighborhood degree δ_u; they are denoted with the prefix "N" (NGA, NM_1, ...).

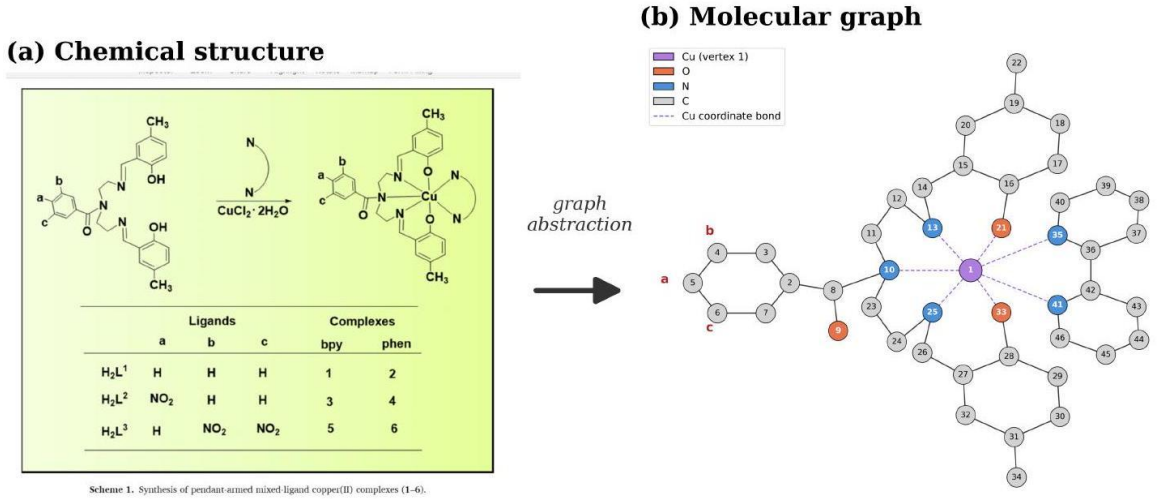

Figure 1. Conversion of the chemical structure of the mixed-ligand copper(II) complex into its molecular graph (complex 1).Conversion of the chemical structure of the pendant-armed mixed-ligand copper(II) complex into its hydrogen-suppressed molecular graph (complex 1, $[CuL^1(bpy)], |V| = 46, |E| = 55$): heavy atoms are vertices and bonds are edges, including the seven Cu-O/Cu-N coordinate bonds (dashed). Positions a, b, c carry the NO_2 groups in complexes 3-6; complexes 2, 4, 6 replace bipyridyl by 1,10-phenanthroline.

Table 1. Degree-based topological indices. The neighborhood versions replace d_u by $\delta_u = \sum_{v \in N(u)} d_v$.

Index	Symbol	Definition
Geometric-Arithmetic	GA	$\sum_{uv \in E} \frac{2\sqrt{d_u d_v}}{d_u + d_v}$
Atom-Bond Connectivity	ABC	$\sum_{uv \in E} \sqrt{\frac{d_u + d_v - 2}{d_u d_v}}$
First Zagreb	M_1	$\sum_{uv \in E} (d_u + d_v)$

Natural Resources for Human Health
eISSN: 2583-1194

Second Zagreb	M_2	$\sum_{uv\in E} d_u d_v$
Randić	R	$\sum_{uv\in E} \frac{1}{\sqrt{d_u d_v}}$
Reciprocal Randić	RR	$\sum_{uv\in E} \sqrt{d_u d_v}$
Hyper-Zagreb	HP	$\sum_{uv\in E} (d_u + d_v)^2$
Harmonic	HM	$\sum_{uv\in E} \frac{2}{d_u + d_v}$
Augmented Zagreb	AZI	$\sum_{uv\in E} \left(\frac{d_u d_v}{d_u + d_v - 2}\right)^3$
Sombor	SO	$\sum_{uv\in E} \sqrt{d_u^2 + d_v^2}$
Reduced Sombor	RSO	$\sum_{uv\in E} \sqrt{(d_u - 1)^2 + (d_v - 1)^2}$

For an index $X = \sum_{uv\in E} \phi(u, v)$, the associated Shannon graph entropy is

$$\mathrm{ENT}_X(G) = \log_{10} X - \frac{1}{X} \sum_{uv\in E} \phi(u, v) \log_{10}(\phi(u, v)),$$

which measures the heterogeneity of the edge contributions to X.

3. THE COMPLEXES AND THEIR MOLECULAR GRAPHS

The six complexes are heteroleptic copper(II) species of general formula [CuL(diimine)], in which a pendant-armed dianionic phenolate Schiff-base ligand (L^{1-3}) and a neutral diimine co-ligand (2,2'-bipyridyl, bpy, or 1,10-phenanthroline, phen) complete a pentagonal-bipyramidal copper environment. The ligands differ in the nitro substitution of the benzamide pendant arm: H_2 L^1 (unsubstituted), H_2 L^2 (mono-nitro) and H_2 L^3 (di-nitro). Table 2 lists the composition of each complex together with the order $|V|$ and size $|E|$ of its molecular graph.

Table 2. Composition and graph parameters of complexes 1-6 (hydrogen-suppressed molecular graphs).

Complex	Formula	Co-ligand / arm	$\|V\|$	$\|E\|$
1	[CuL^1 (bpy)], $C_{37}H_{35}N_5O_3Cu$	bpy, benzamide	46	55
2	[CuL^1 (phen)], $C_{39}H_{37}N_5O_3Cu$	phen, benzamide	48	58
3	[CuL^2 (bpy)], $C_{37}H_{36}N_6O_5Cu$	bpy, 4-nitro	47	56
4	[CuL^2 (phen)], $C_{39}H_{36}N_6O_5Cu$	phen, 4-nitro	49	59
5	[CuL^3 (bpy)], $C_{37}H_{35}N_7O_7Cu$	bpy, 3,5-dinitro	48	57

6	$[CuL^3(\text{ phen })], C_{39}H_{35}\ N_7O_7Cu$	phen, 3,5-dinitro	50	60

The complete neighborhood-degree edge partition of the six graphs is given in Table 3; each class (δ_u, δ_v) collects the edges whose end-vertices have the stated neighborhood degrees. Summation of the appropriate edge weight over this partition yields every neighborhood index in closed form; the values so obtained (Table 5) reproduce the reported data exactly.

Table 3. Neighbourhood-degree edge partition (δ_u, δ_v) of complexes 1-6 (entries are edge multiplicities; "_" denotes an absent class).

(δ_u, δ_v)	**1**	**2**	**3**	**4**	**5**	**6**
(3,5)	2	2	3	3	4	4
(3,8)	1	1	1	1	1	1
(4,4)	4	2	2	-	2	-
(4,5)	6	6	4	4	4	4
(5,5)	4	5	8	9	4	5
(5,6)	4	4	4	4	8	8
(5,7)	4	8	4	8	2	6
(5,8)	2	-	2	-	2	-
(5,11)	2	2	2	2	2	2
(5,12)	2	2	2	2	2	2
(6,7)	4	4	4	4	6	6
(6,11)	2	2	2	2	2	2
(6,14)	2	2	2	2	2	2
(7,7)	2	2	2	2	2	2
(7,8)	1	1	1	1	1	1
(7,9)	-	2	-	2	-	2
(7,10)	2	2	2	2	2	2
(8,8)	1	-	1	-	1	-
(8,12)	2	-	2	-	2	-
(8,14)	1	1	1	1	1	1
(9,9)	-	1	-	1	-	1
(9,12)	-	2	-	2	-	2
(10,20)	2	2	2	2	2	2
(11,20)	2	2	2	2	2	2

(12,20)	2	2	2	2	2	2
(14,20)	1	1	1	1	1	1
Total edges	55	58	56	59	57	60

4 RESULTS AND DISCUSSION

4.1 Degree-based topological indices

The eleven ordinary degree-based indices are collected in Table 4. All indices increase monotonically along the two structural axes of the series: within a fixed co-ligand they rise with the number of nitro groups ($\mathbf{1 \rightarrow 3 \rightarrow 5}$ for bpy; $\mathbf{2 \rightarrow 4 \rightarrow 6}$ for phen), and for a fixed pendant arm the phenanthroline complexes exceed their bipyridyl analogues, consistent with the larger fused aromatic system of Phen.

Table 4. Degree-based topological indices of complexes 1-6.

Complex	GA	ABC	M_1	M_2	R	RR	HP	HM	AZI	SO	RSO
1	53.32	38.42	302	419	22.31	145.31	1842	21.68	514.76	220.89	146.07
2	56.28	40.46	320	445	23.29	154.21	1948	22.65	545.54	233.76	154.78
3	54.15	39.23	308	426	22.70	147.94	1876	21.98	518.13	225.61	149.71
4	57.11	41.27	326	452	23.68	156.84	1982	22.95	548.91	238.48	158.42
5	54.97	40.05	314	433	23.09	150.57	1910	22.28	521.51	230.33	153.35
6	57.93	42.09	332	459	24.08	159.47	2016	23.25	552.29	243.19	162.07

4.2 Neighborhood topological indices

The neighborhood indices computed from the edge partition of Table 3 are given in Table 5 and displayed in Fig. 2. They follow the same ordering as the degree-based indices but are numerically larger, because each edge is weighted by the neighborhood degrees δ_u, δ_v and therefore encodes information from the second coordination sphere.

Table 5. Neighbourhood-degree-based topological indices of complexes 1-6 (derived from Table 3).

Cm	NGA	NABC	NM_1	NM_2	NR	NRR	NHP	NHM	NAZI	NSO	NRSO
1	53.68	28.13	838	3638	8.74	406.59	15594	8.57	5939.32	609.18	533.30
2	56.68	29.45	890	3858	9.03	432.67	16466	8.85	6287.62	645.85	565.73
3	54.66	28.61	852	3681	8.85	413.52	15768	8.67	5992.44	619.18	541.91
4	57.66	29.94	904	3901	9.14	439.59	16640	8.96	6340.74	655.85	574.34
5	55.64	29.13	866	3730	9.01	420.43	15966	8.83	6059.72	629.20	550.57

6	58.64	30.45	918	3950	9.30	446.51	16838	9.11	6408.02	665.87	582.99

To illustrate how Table 5 is obtained from Table 3, consider the edge class (5,7) of complex 1, which has multiplicity 4. Each such edge contributes NGA = $2\sqrt{(5\times7)}/(5+7) \approx 0.7638$, so the four edges together add $4 \times 0.7638 \approx 3.055$ to NGA(1); summing this contribution across all 26 edge classes of complex 1 reproduces the reported NGA = 53.68 in Table 5 exactly. The same procedure, applied edge-class by edge-class, generates every entry of Tables 4–6 from the partition in Table 3.

Figure 2. Neighborhood topological indices of complexes 1-6 on a logarithmic scale.

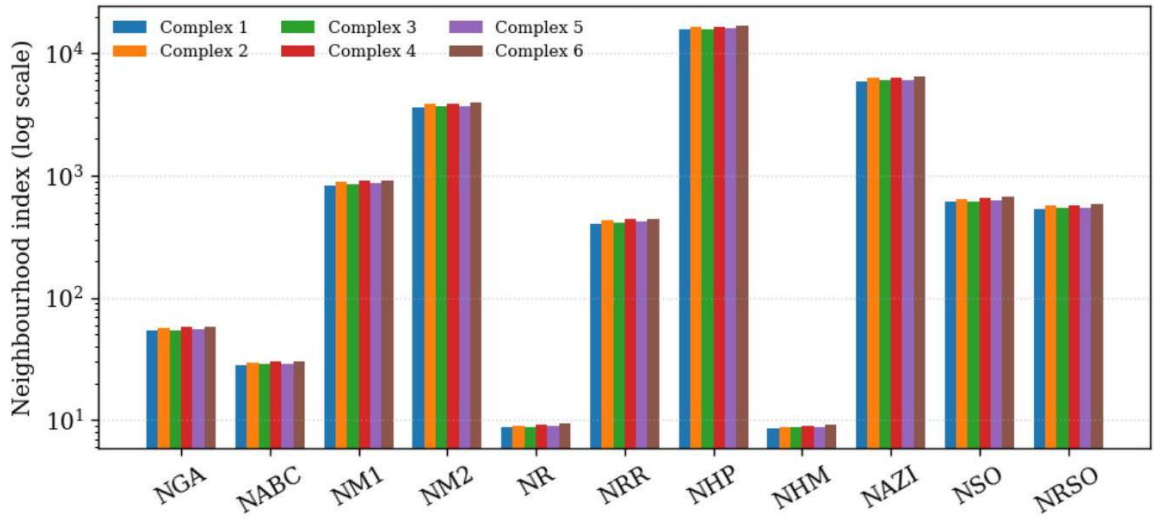

4.3 Neighborhood graph entropy

The Shannon entropies of the neighborhood indices (Table 6, Fig. 3) lie in the range 1.47-1.78, confirming that the six complexes share a common structural skeleton and differ only in local substitution. Within this narrow range the entropy nevertheless increases systematically from 1 to 6, so the entropy descriptors preserve the ordering of the complexes; the AZI-weighted entropy shows the widest spread and is the most discriminating.

Table 6. Shannon entropy of the neighborhood indices $(\log_{10})$.

Cm	GA	ABC	M_1	M_2	R	RR	HP	HM	AZI	SO	RSO
1	1.7402	1.7351	1.6977	1.5734	1.7115	1.7000	1.5671	1.7097	1.4717	1.6954	1.6816
2	1.7632	1.7585	1.7239	1.6063	1.7366	1.7259	1.5999	1.7351	1.5083	1.7217	1.7090
3	1.7480	1.7431	1.7067	1.5836	1.7208	1.7090	1.5771	1.7192	1.4813	1.7044	1.6911
4	1.7707	1.7661	1.7324	1.6158	1.7455	1.7344	1.6093	1.7442	1.5174	1.7302	1.7180
5	1.7557	1.7508	1.7150	1.5930	1.7284	1.7171	1.5865	1.7270	1.4912	1.7128	1.6996
6	1.7780	1.7733	1.7401	1.6246	1.7526	1.7421	1.6181	1.7515	1.5266	1.7381	1.7260

Figure 3. Representative neighborhood graph entropies across complexes 1-6

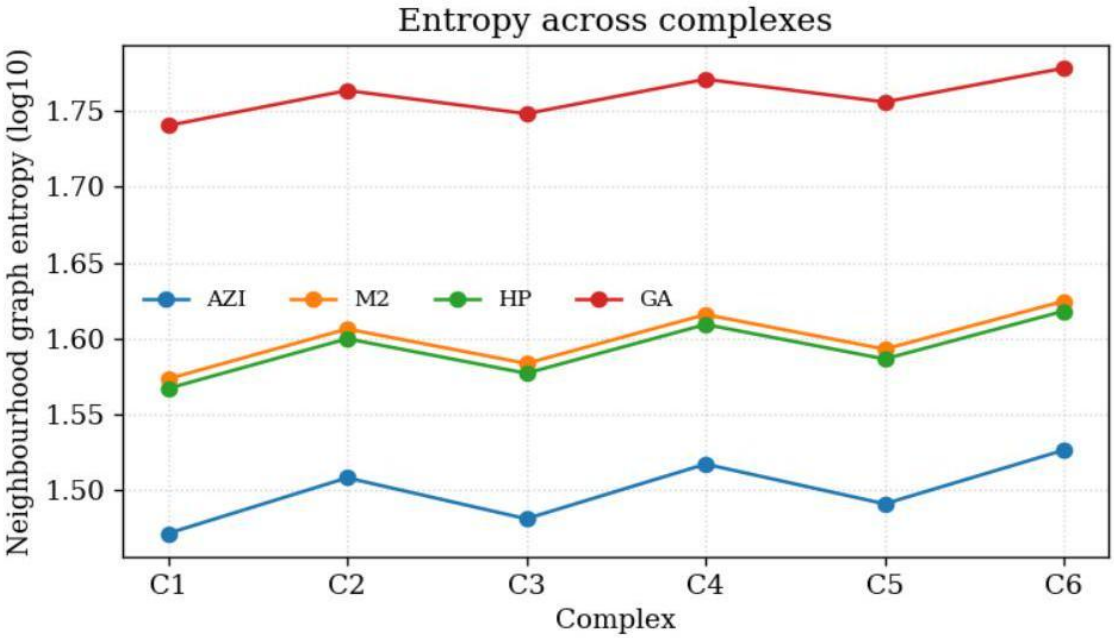

4.4 QSPR: antibacterial activity

The experimental antibacterial activity of the complexes, expressed as the zone of inhibition (mm) against five Gram-negative and three Gram-positive strains, is reproduced in Table 7. The mean response ranks the complexes as **4 > 6 > 2 > 3 > 1 > 5**, the phenanthroline complexes being the more active on average.

Table 7. Antibacterial activity (zone of inhibition, mm) of complexes 1-6. Strain codes: P.a (Pseudomonas aeruginosa), P.v (Proteus vulgaris), S.d (Shigella dysenteriae), K.p (Klebsiella pneumoniae), E.coli, S.a (Staphylococcus aureus), B.s (Bacillus subtilis), S.e (Staphylococcus epidermidis).

Complex	P.a	P.v	S.d	K.p	E.coli	S.a	B.s	S.e	Mean
1	22	21	23	22	20	22	18	19	20.88
2	28	28	20	25	23	29	26	23	25.25
3	24	25	25	19	15	25	21	17	21.38
4	29	29	27	22	22	27	27	26	26.12
5	19	25	25	19	15	25	20	18	20.75
6	24	26	29	24	28	27	25	25	26.00

A linear regression of each activity on each descriptor was performed; the resulting Pearson coefficients for the degree-based indices are mapped in Fig. 4. The correlations are uniformly positive and strong, particularly for the Gram-positive strains and E. coli. Because the strains respond in a strongly correlated manner, the mean zone of inhibition was adopted as a single robust activity variable. Table 8 lists, for each family of descriptors, the coefficient of determination R^2, the leave-one-out

cross-validated Q^2_{LOO} and the significance p of the regression of the mean activity on the best descriptor. In every family the Augmented Zagreb Index is the leading descriptor.

Figure 4. Pearson correlation coefficients between the degree-based indices and the antibacterial activity against each strain.

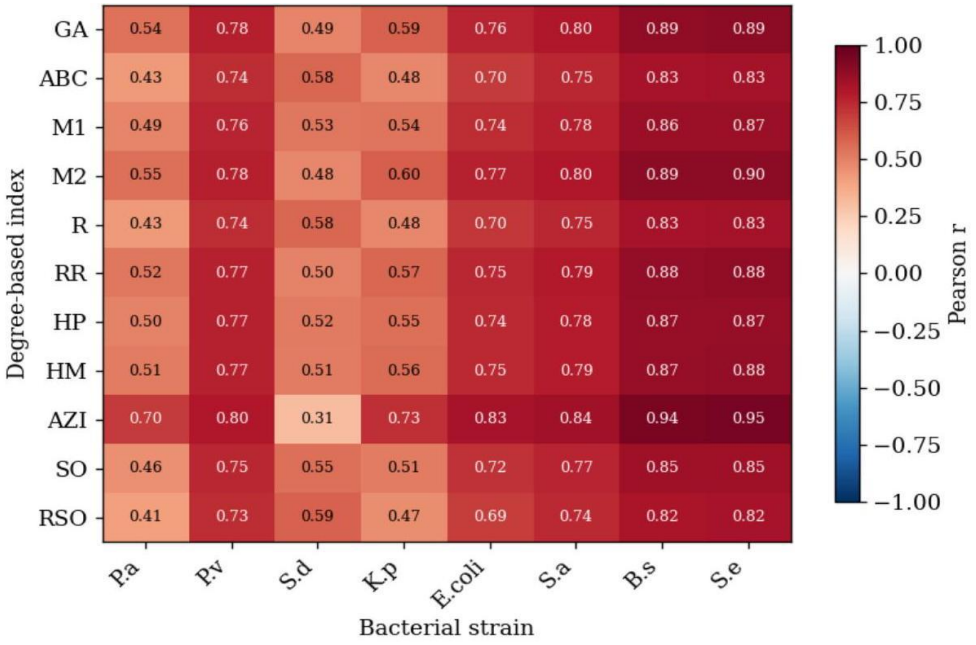

Table 8. Leading single-descriptor QSPR models for the mean antibacterial activity, by descriptor family $(n = 6)$.

Family	Best index	R^2	Q^2_{LOO}	p
Degree-based	AZI	0.969	0.934	0.0004
Neighbourhood	NAZI	0.932	0.860	0.0018
Entropy	AZI-entropy	0.865	0.760	0.0072

The leave-one-out procedure removed each complex in turn, refit the regression on the remaining five, and predicted the omitted value; Q^2LOO is the resulting cross-validated coefficient of determination. The thresholds $R^2 > 0.6$ and $Q^2 > 0.5$ follow the conventional acceptance criteria used in QSPR/QSAR practice (e.g. Golbraikh and Tropsha, J. Mol. Graph. Model. 2002). Comparing the three families directly, the degree-based descriptor (AZI, $R^2 = 0.969$) outperforms the neighbourhood descriptor (NAZI, $R^2 = 0.932$) and the entropy descriptor (AZI-entropy, $R^2 = 0.865$), indicating that raw connectivity information is only partially degraded when re-expressed as a second-sphere or entropy-based quantity for this series.

The optimal model relates the mean antibacterial activity to the degree-based Augmented Zagreb Index (Fig. 5):

$$(\overline{\mathrm{ZOI}})_{\mathrm{mm}} = 0.1523(\mathrm{AZI}) - 57.85,$$
$$n = 6, R^2 = 0.969, R^2_{\mathrm{adj}} = 0.961, F = 123.9, p = 0.0004, Q^2_{\mathrm{LOO}} = 0.934.$$

The observed and cross-validated predicted activities agree to within 0.9 mm for every complex (Fig. 6), so the model comfortably satisfies the usual acceptance thresholds $(R^2 > 0.6, Q^2 > 0.5)$.

Figure 5. Best QSPR model: mean antibacterial activity versus the Augmented Zagreb Index of complexes 1-6.

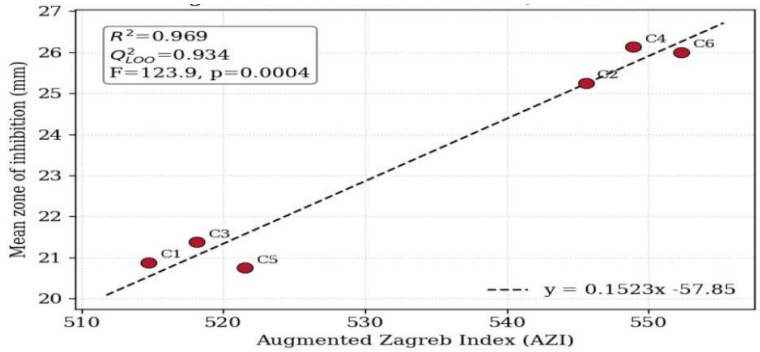

Figure 6. Observed versus leave-one-out predicted mean antibacterial activity for the AZI model (dashed line $y = x$).

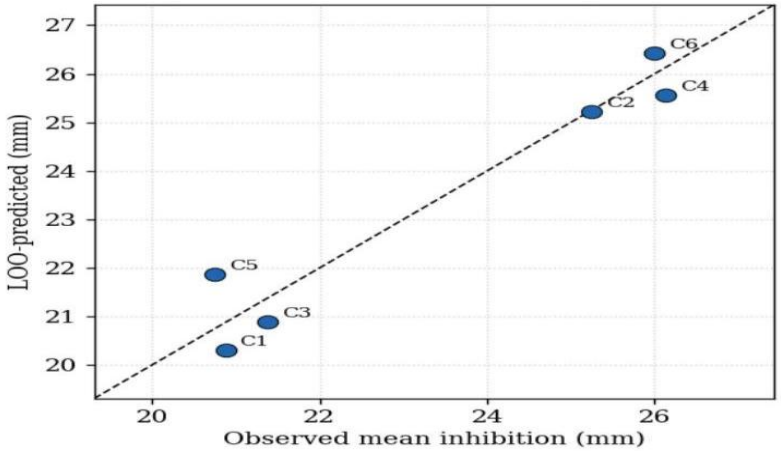

4.5 QSPR: SARS-CoV-2 docking affinity

The reported molecular-docking study places the six complexes against the SARS-CoV-2 receptor with estimated binding free energies ΔG from -8.85 to $-11.81\text{kcalmol}^{-1}$ and inhibition constants K_i in the nanomolar range (Table 9), all more favourable than the reference drugs chloroquine and molnupiravir. Regressing the binding affinity ($-\Delta G$) on the descriptors gives strong linear relationships, but here the size-type descriptors ($M_1, \text{HP}, \text{SO}$) outperform AZI, with $R^2 \approx 0.78 (p < 0.02)$. The best model,

$$(-\Delta G)_{\text{kcal/mol}} = 0.0889(M_1) - 17.60, R^2 = 0.785, p = 0.019,$$

is shown in Fig. 7; essentially the same fit is obtained for the inhibition potency $\text{p}K_i$. This contrast is chemically sensible: the antibacterial response is governed by the branching/lipophilicity that AZI emphasises, whereas the receptor binding scales more nearly with overall molecular size, which the first-Zagreb and hyper-Zagreb indices capture.

Table 9. SARS-CoV-2 molecular-docking parameters of complexes 1-6 (from the base study).

Complex	$\Delta G(\text{kcalmol}^{-1})$	$K_i(\text{nM})$
1	-8.85	326.35
2	-11.11	7.13
3	-9.54	100.84
4	-11.81	2.20

5	-10.91	9.91
6	-11.18	6.36

Figure 7. QSPR model relating the SARS-CoV-2 binding affinity ($-\Delta G$) to the first Zagreb index M_1 of complexes 1-6.

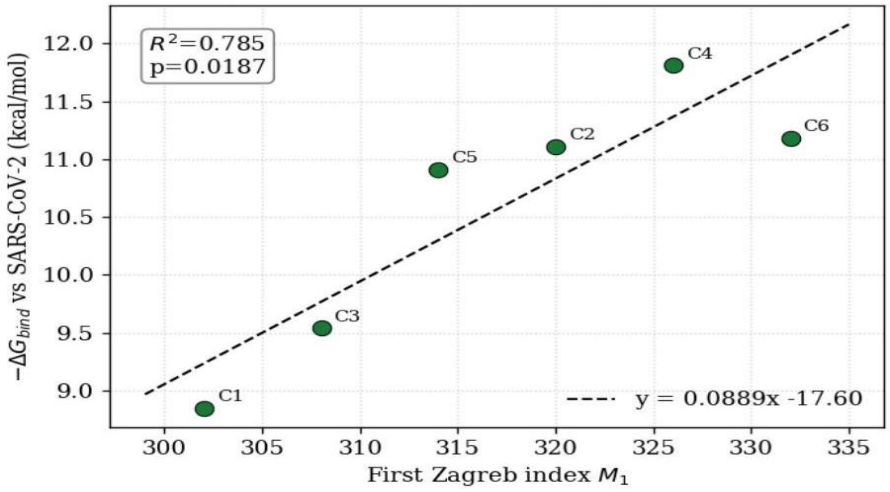

4.6 Relationship to DNA binding and limitations

The reported DNA-binding propensity of the complexes, $\mathbf{6 > 4 > 2 > 5 > 3 > 1}$ (intrinsic binding constants $K_b \approx 3.8 - 5.1 \times 10^4 \mathrm{M}^{-1}$), tracks the descriptor ordering closely: the two most strongly DNAbinding complexes, 6 and 4, also carry the largest index values, consistent with the additional aromatic surface of phenanthroline and the electron-withdrawing nitro groups promoting groove binding. Individual K_b values were not available for a formal regression and this relationship is therefore reported qualitatively.

Two limitations should be stated. First, the descriptors within each family are strongly mutually correlated, so the QSPR results are best read as a ranking of single descriptors rather than as independent structural effects; multivariate models on six compounds would be over-parameterised and were not attempted. Second, with $n = 6$ the statistical power is limited, so the cross-validated models are best regarded as screening tools to be re-fitted as further members of the series become available.

The models were also not tested against an external validation set of complexes outside the present series; the reported R^2 and Q^2LOO values should therefore be read as internal-validation performance only, and independent testing on new complexes is recommended before the models are used prospectively.

5. CONCLUSION

The molecular graphs of six pendant-armed mixed-ligand copper(II) complexes were constructed, their complete neighbourhood-degree edge partitions determined, and eleven neighborhood topological indices, the ordinary degree-based indices and the neighborhood graph entropies evaluated; the edge partitions reproduce the reported indices exactly. A multi-target QSPR analysis showed that the Augmented Zagreb Index is the strongest single predictor of the mean antibacterial activity ($R^2 = 0.969, Q^2_{\mathrm{LOO}} = 0.934$, while the size-type indices M1 and HP best reproduce the SARS-CoV-2 docking affinity $(R^2 \approx 0.78)$, and the descriptor ordering is consistent with the reported DNA-binding propensity. Topological indices thus provide a rapid, structure-only route for ranking the multi-target antibacterial activity and SARS-CoV-2 docking affinity of this family of copper(II) metallodrugs and for guiding the design of related complexes.

ACKNOWLEDGEMENTS

The authors also thank the corresponding authors of the base experimental study [23] for the published antibacterial, DNA-binding, and molecular-docking data on which the present QSPR analysis is built.

AUTHOR CONTRIBUTIONS

Mythili V: Conceptualization, Methodology, Software, Writing-original draft.

S Shenbaga Devi: Formal Analysis, Validation.

Padmanathan Arthi: Data Curation, Resources.

S Dhanalakshmi: Supervision, Review & Editing.

CONFLICT OF INTEREST

The authors declare that there is no conflict of interest.

ETHICS STATEMENT

The antibacterial activity and molecular-docking data analyzed here were obtained from a previously published, ethically approved study (Arthi et al., *Chem. Biol. Interact.* 373 (2023) 110349) and are used with appropriate citation. No new ethical approval was required for the present work.

DATA AVAILABILITY STATEMENT

The topological index values, edge partitions, and QSPR model outputs generated in this study are included within the article (Tables 1–9). The underlying experimental antibacterial activity and SARS-CoV-2 docking data were sourced from the previously published study by Arthi et al. (2023) [23]. Any computational scripts used to derive the indices are available from the corresponding author upon reasonable request.

REFERENCES

[1] H. Wiener, Structural determination of paraffin boiling points, *J. Am. Chem. Soc.* 69 (1947) 17–20. doi:10.1021/ja01193a005.

[2] I. Gutman, N. Trinajstic´, Graph theory and molecular orbitals. Total π-electron energy of alternant hydro-carbons, *Chem. Phys. Lett.* 17 (1972) 535–538. doi:10.1016/0009-2614(72)85099-1.

[3] M. Randic´, Characterization of molecular branching, *J. Am. Chem. Soc.* 97 (1975) 6609–6615. doi:10.1021/ja00856a001.

[4] E. Estrada, L. Torres, L. Rodr´ıguez, I. Gutman, An atom–bond connectivity index, *Indian J. Chem.* 37A (1998) 849–855.

[5] D. Vukic˘evic´, B. Furtula, Topological index based on the ratios of geometrical and arithmetical means of end-vertex degrees of edges, *J. Math. Chem.* 46 (2009) 1369–1376. doi:10.1007/s10910-009-9520-x.

[6] B. Furtula, A. Graovac, D. Vukic˘evic´, Augmented Zagreb index, *J. Math. Chem.* 48 (2010) 370–380. doi:10.1007/s10910-010-9677-3.

[7] I. Gutman, Geometric approach to degree-based topological indices: Sombor indices, *MATCH Commun. Math. Comput. Chem.* 86 (2021) 11–16.

[8] V. Kumar, S. Das, A novel approach to determine the Sombor-type indices via M-polynomial, *J. Appl. Math. Comput.* 71 (2025) 983–1007. doi:10.1007/s12190-024-02272-4.

[9] X. Zhang, S. Noureen, S. Kamran, S. M. Ibrahim, A. Aslam, Sombor indices in main group metal chem-istry: computational evaluation of bismuth(III) iodide, oxide/silicate frameworks, and dendrimers for QSAR applications, *Main Group Met. Chem.* 48 (2025) 20250011. doi:10.1515/mgmc-2025-0011.

[10] S. Mondal, N. De, A. Pal, On some new neighbourhood degree-based indices, *Acta Chem. Iasi* 27 (2019) 31–46.

[11] A. Sivaranjani, S. Radha, QSPR analysis of anti-HIV drugs using neighborhood degree sum-based topolog-ical indices, *Eur. Phys. J. E* 48 (2025) 68. doi:10.1140/epje/s10189-025-00534-y.

[12] D. Balasubramaniyan, N. Chidambaram, On some neighbourhood degree-based topological indices with QSPR analysis of asthma drugs, *Eur. Phys. J. Plus* 138 (2023) 823. doi:10.1140/epjp/s13360-023-04439-7.

[13] M. Irfan, F. Yasmeen, S. Aziz, M. Mukhtar, Neighborhood degree-based topological indices of nanotube via direct and NM-polynomial, *Int. J. Quantum Chem.* 124 (2024) e27474. doi:10.1002/qua.27474.

[14] S. Das, S. Rai, V. Kumar, On topological indices of Molnupiravir and its QSPR modelling with some other antiviral drugs to treat COVID-19 patients, *J. Math. Chem.* 62 (2024) 2581–2624. doi:10.1007/s10910-023-01518-z.

[15] M. Dehmer, Information processing in complex networks: graph entropy and information functionals, *Appl. Math. Comput.* 201 (2008) 82–94.

[16] M. A. Malik, M. Imran, M. Adeel, On distance-based topological indices and co-indices of fractal-type molecular graphs and their respective graph entropies, *PLoS ONE* 18 (2023) e0290047. doi:10.1371/journal.pone.0290047.
[17] R. Huang, A. Mahboob, M. W. Rasheed, S. M. Alam, M. K. Siddiqui, On molecular modeling and QSPR analysis of Lyme disease medicines via topological indices, *Eur. Phys. J. Plus* 138 (2023) 243. doi:10.1140/epjp/s13360-023-03867-9.
[18] V. Ravi, QSPR analysis of drugs used for treatment of hepatitis via reduced reverse degree-based topological descriptors, *Phys. Scr.* 99 (2024) 105236. doi:10.1088/1402-4896/ad729d.
[19] A. Mahboob, M. W. Rasheed, A. M. Dhiaa, I. Hanif, L. Amin, On QSPR analysis of physicochemical properties and anti-hepatitis prescription drugs using a linear regression model, *Heliyon* 10 (2024) e25908. doi:10.1016/j.heliyon.2024.e25908.
[20] N. U. H. Awan et al., QSPR analysis for physiochemical properties of new potential antimalarial compounds involving topological indices, *Int. J. Quantum Chem.* 124 (2024) e27391. doi:10.1002/qua.27391.
[21] M. W. Rasheed, A. Mahboob, I. Hanif, Uses of degree-based topological indices in QSPR analysis of alka-loids with poisonous and healthful nature, *Front. Phys.* 12 (2024) 1381887. doi:10.3389/fphy.2024.1381887.
[22] Y. Tu, S. Yousaf, S. Tariq et al., Computational analysis of metal–organic framework and covalent–organic framework using degree-based topological indices with QSPR validation, *Sci. Rep.* 15 (2025)37311. doi:10.1038/s41598-025-21240-x.
[23] P. Arthi, M. Dharmasivam, B. Kaya, A. Kalilur Rahiman, Multi-target activity of copper complexes: an-tibacterial, DNA binding, and molecular docking with SARS-CoV-2 receptor, *Chem. Biol. Interact.* 373 (2023) 110349. doi:10.1016/j.cbi.2023.110349.
[24] S. Shenbaga Devi, S. Dhanalakshmi, Analysis of degree-based topological indices for stroke treatment drugs: a study on the physicochemical features, *IAENG Int. J. Appl. Math.* 54 (2024) 1233–1239.
[25] S. Shenbaga Devi, S. Dhanalakshmi, Quantitative structure–property relationship-based analysis of topological indices for antihypertensive drugs, *Math. Model. Eng. Probl.* 12 (2025) 3094–3102. doi:10.18280/mmep.120913.